# Photoinduced swing of a diarylethene thin broad sword shaped crystal, A study on the detailed mechanism

Ayako Fujimoto,[a] Noriko Fujinaga,[a] Ryo Nishimura,[a] Eri Hatano,[a] Luna Kono,[a] Akira Nagai,[a] Akiko Sekine,[b] Yohei Hattori,[a] Yuko Kojima,[c] Nobuhiro Yasuda,[d] Masakazu Morimoto,[e] Satoshi Yokojima,[f] Shinichiro Nakamura,[g] Ben L. Feringa,[h] and Kingo Uchida[a *]

a. Department of Materials Chemistry, Faculty of Science and Technology, Ryukoku University, Seta, Otsu, Shiga 520-2194, Japan, Fax: +81-77-543-7483; Tel: +81-77-543-7462; E-mail: uchida@rins.ryukoku.ac.jp

b. Department of Chemistry, School of Science, Tokyo Institute of Technology, Ookayama 2-12-1, Meguro-ku, Tokyo 152-8551, Japan

c. Materials Characterization Laboratory, Mitsubishi Chemical Corporation 1000, Kamoshida-cho, Aoba-ku, Yokohama 227-8502, Japan

d. Japan Synchrotron Radiation Research Institute, 1-1-1 Kouto, Sayo-cho, Sayo-gun, Hyogo 679-5198 Japan

e. Department of Chemistry and Research Center for Smart Molecules, Rikkyo University, Nishi-Ikebukuro 3-34-1, Toshima-ku, Tokyo 171-8501, Japan

f. Tokyo University of Pharmacy and Life Science, Horino-uchi 1432-1, Hachioji, Tokyo 192-0392, Japan

g. Nakamura Laboratory, RIKEN Cluster for Science, Technology and Innovation Hub, 2-1 Hirosawa, Wako, Saitama 351-0198 Japan

h. Stratingh Institute for Chemistry, University of Groningen, Nijenborgh 4, 9747 AG Groningen, The Netherlands; Fax: +31-50-363-4296; E-mail: b.l.feringa@rug.nl

**Supporting Information**

**Table of Contents:**

**Preparation of thin broad sword shaped crystals of 1oRR**

A diarylethene derivative **1oRR** was prepared according to the previous paper.[1] Thin broad sword shaped crystals of **1oRR** were obtained by sublimation at 250 °C, which is 20 °C below the melting point of the compound. Molecular packing of these crystals was the same as the one in previous paper,[2] and the distances of the reactive carbon atoms were less than 4.2 Å indicating they are reactive in crystalline state.[3]

**Table S1.** Crystal data of thin broad sword shaped (monoclinic) crystals and block crystals of **1oRR** and block ones of **1cRR**.

| | Thin crystal of **1oRR** | Block crystal of **1oRR** | **1cRR** |
|---|---|---|---|
| Method | Sublimation | Recrystallization from MeOH | |
| $T$ / K | 173 (2) | 173 (2) | 173 (2) |
| crystal system | monoclinic | monoclinic | tetragonal |
| space group | $P2_1$ | $P2_1$ | $P4_3$ |
| $a$ / Å | 12.3940 (9) | 12.3769 (5) | 13.253 (3) |
| $b$ / Å | 14.5843 (5) | 14.6220 (6) | 13.253 (3) |
| $c$ / Å | 19.4720 (7) | 19.3798 (8) | 19.0733 (18) |
| $\alpha$ / ° | 90 | 90 | 90 |
| $\beta$ / ° | 107.233 (4) | 106.751 (7) | 90 |
| $\gamma$ / ° | 90 | 90 | 90 |
| $V$ / Å$^3$ | 3361.7 (3) | 3358.4 (3) | 3350.1 (15) |
| $Z$ | 4 | 4 | 4 |
| $R_1$ ($I > 2\sigma(I)$) | 0.0779 | 0.0516 | 0.0889 |
| $wR_2$ ($I > 2\sigma(I)$) | 0.1738 | 0.1397 | 0.2700 |
| $R_1$ (all data) | 0.1727 | 0.0561 | 0.0956 |
| $wR_2$ (all data) | 0.2467 | 0.1447 | 0.2797 |
| CCDC | 1938354 | 1938355 | 1961657 |

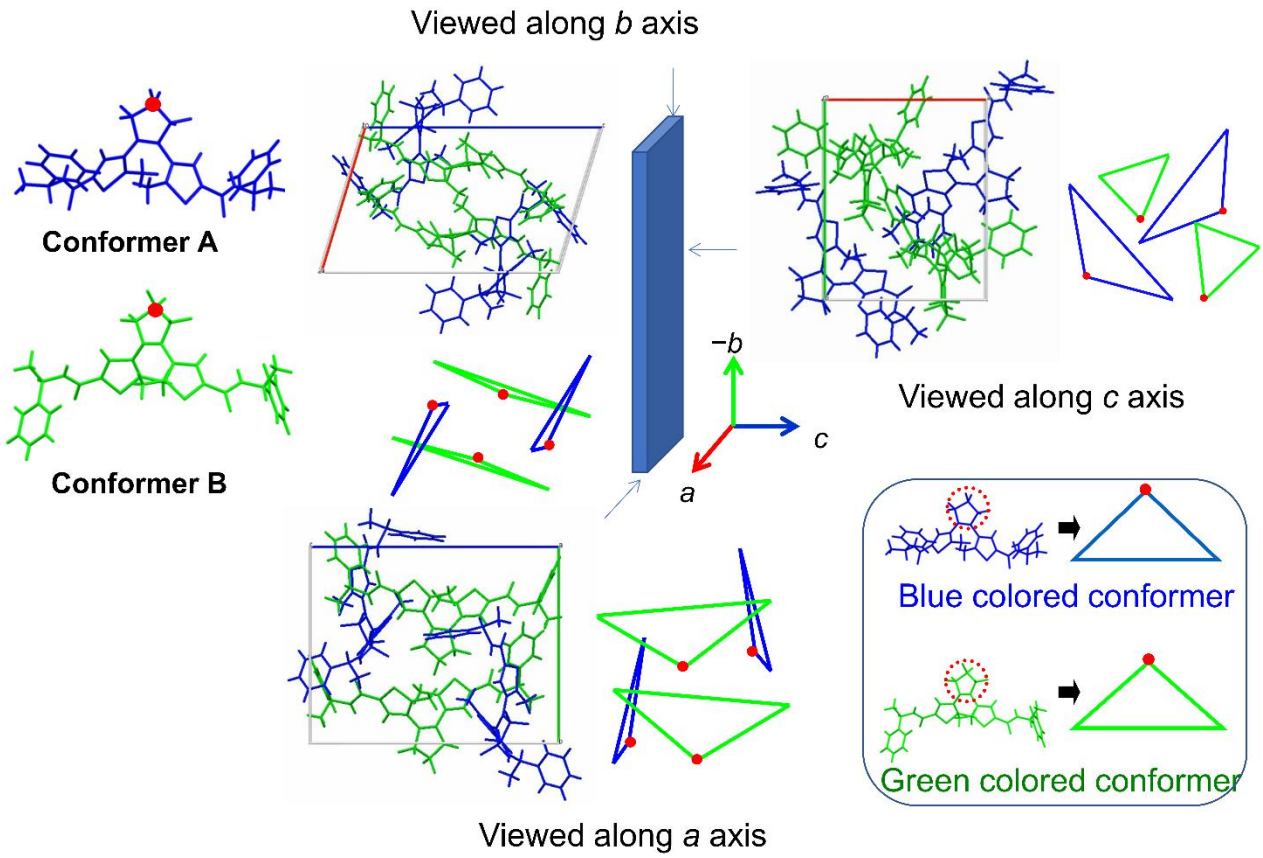


**Figure S1.** Molecular packing of **1oRR** in the crystal. There are two conformers A and B with 1: 1 ratio of **1oRR** molecules in crystal. The conformers A and B are shown in blue and green, respectively. To make it easier to understand the packing of diarylethene molecules, the blue and green colored conformers are indicated by blue triangles and green triangles, respectively. Also, the apex of perfluorocyclopentene is indicated by red dots. Packing observed along *c* axis is the widest face of the crystal. Packing observed along *b* axis is the apex portion of the crystal viewed along *a* axis which is the side face portion of the crystal. Viewed along *b* axis, the blue and green conformers are orthogonal to each other. Viewed along *a* axis, the green conformer shows the widest part of the molecule, whereas the blue conformer is placed perpendicular to the surface. Viewed along *c* axis, contrary to the previous one, the blue conformer shows the widest part of the molecule and the two blue conformers are arranged vertically.

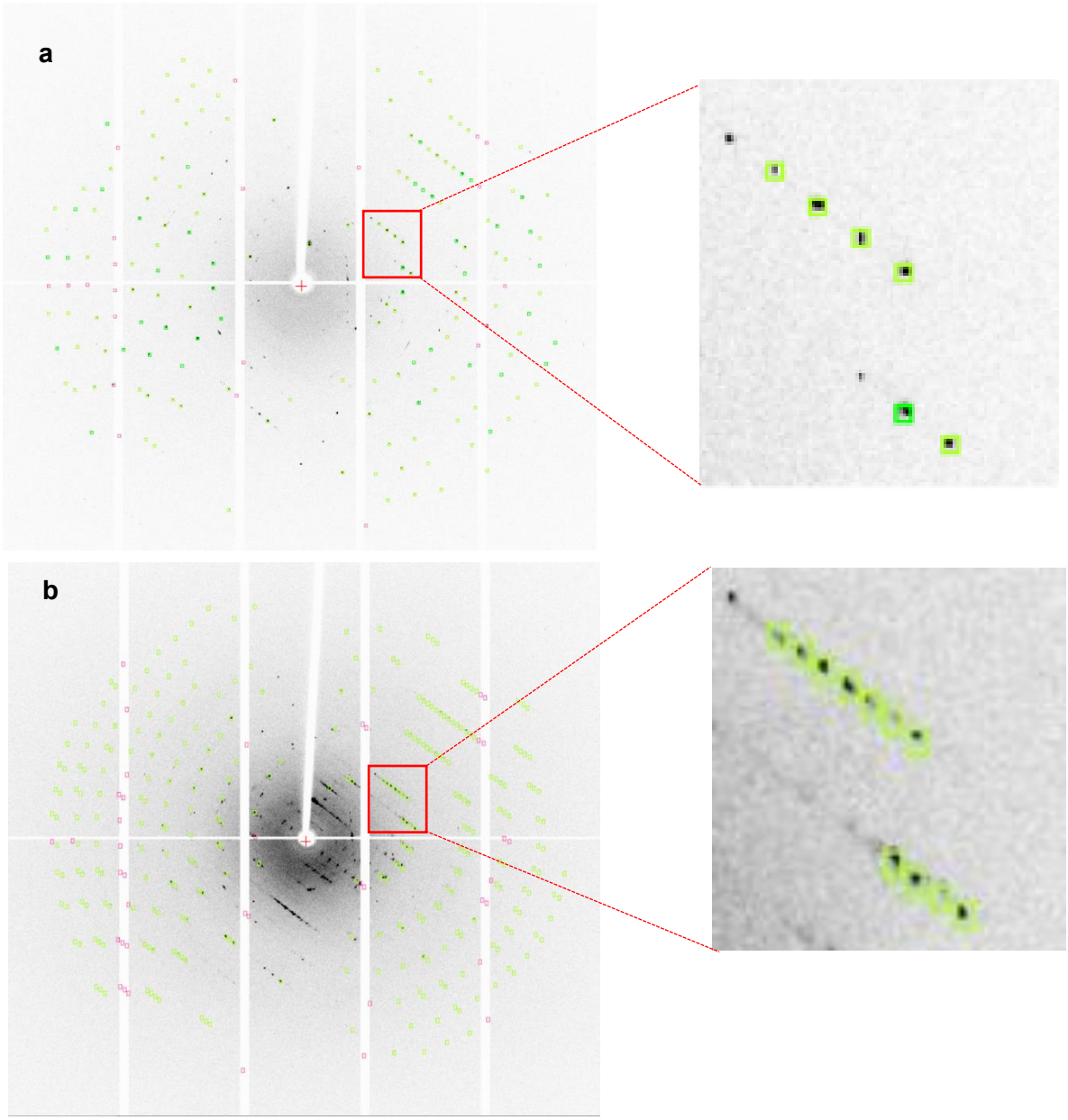


**Figure S2.** Diffraction pattern image of monoclinic block crystals of **1oRR** (a) before and (b) after UV light (313 nm) irradiation for 9 min., respectively. Upon UV light irradiation, the number of diffraction spots approximately doubled. This phenomenon suggested that block crystals of **1oRR** undergo photoinduced SCSC phase transition from phase I to phase $II_{UV}$.

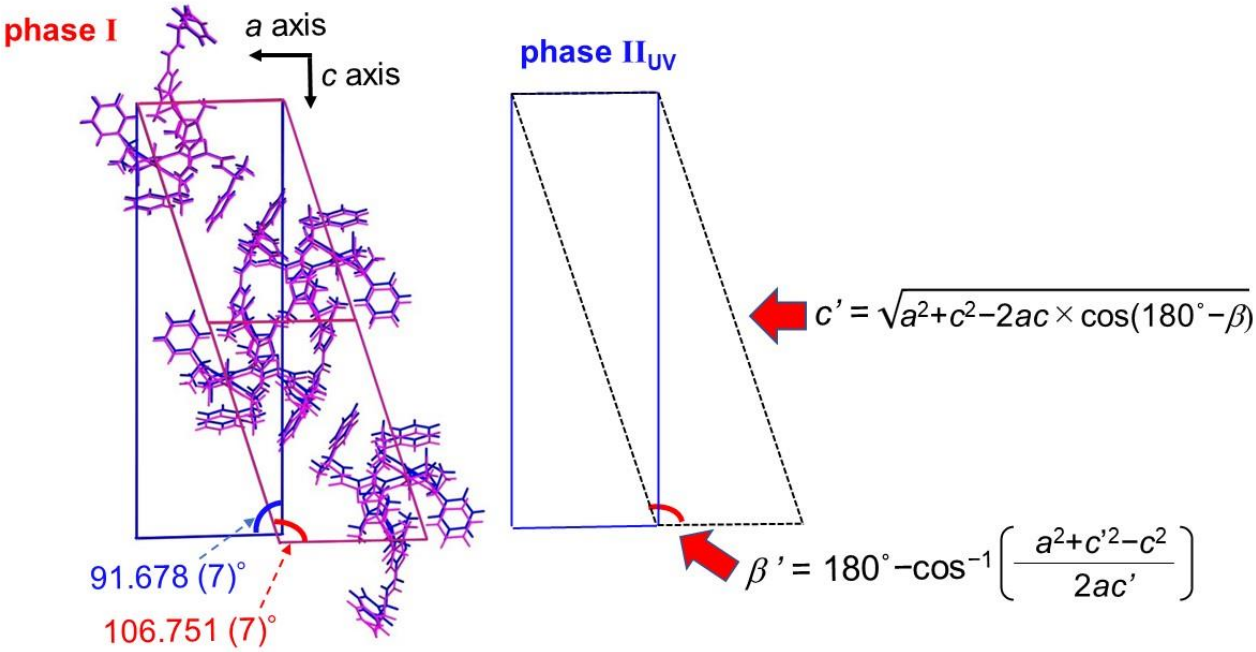


**Figure S3.** Comparison of the lengths of *c* axis and $\beta$ angle at phase transition. In order to compare the cell size before and after the phase transition of monoclinic block crystal of **1oRR**, the length of *c* axis of phase I and the half length of the diagonal length between *c* and *a* axis of phase $II_{UV}$ were compared. Further, the $\beta$'-angle is obtained as an angle formed by the *a* axis and the diagonal line of the *a* and *c* axes in the case of phase $II_{UV}$ and was compared with the $\beta$ angle of phase I.

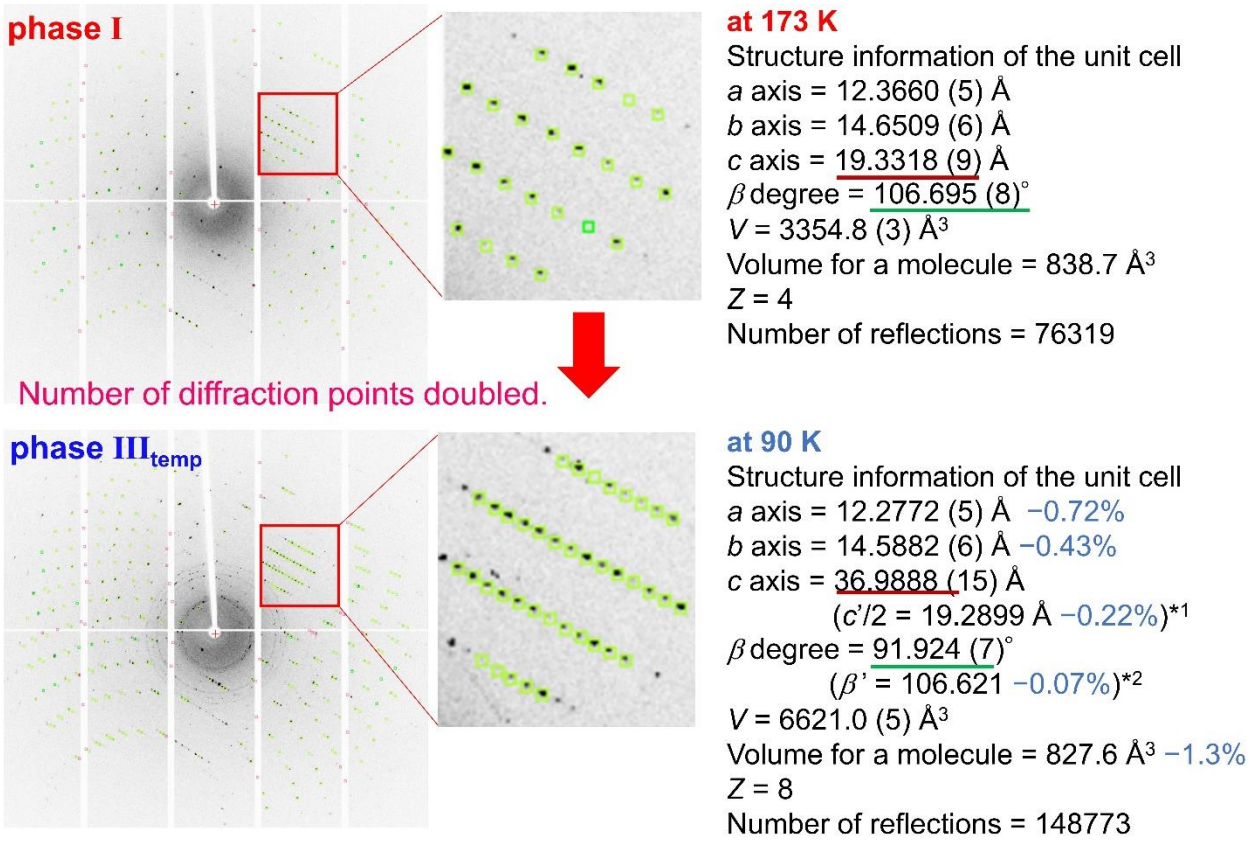


**Figure S4.** Diffraction pattern before and after SCSC phase transition from phase I to phase III$_{temp}$ transition at beamline 40XU of SPring-8. It was found that when measuring at 90 K, which can be measured with beamline 40XU (The lower limit temperature of the beamline is 90 K.), the diffraction spots is doubled from about 76,000 to 149,000 spots. By repeating the process of lowering and raising the temperature between 90 K and 173 K, we observed the same phenomena. We thus confirmed that this is due to the SCSC phase transition. The number of diffraction spots were carefully examined by lowering the temperature at 110 K, however, the crystal analysis was impossible due to the low concentration of diffraction pattern of phase III$_{temp}$ at the temperature.

*1: In order to compare the cell size before and after the phase transition, the half-length of the diagonal length between *c* and *a* axis (*c'* axis) were compared.

*2: The *β'*-angle is obtained as an angle formed by the *a*-axis and the diagonal line of the *a*- and *c*-axes. The angle was compared with the *β*-angle before phase transition. The details are described in Figure S3.

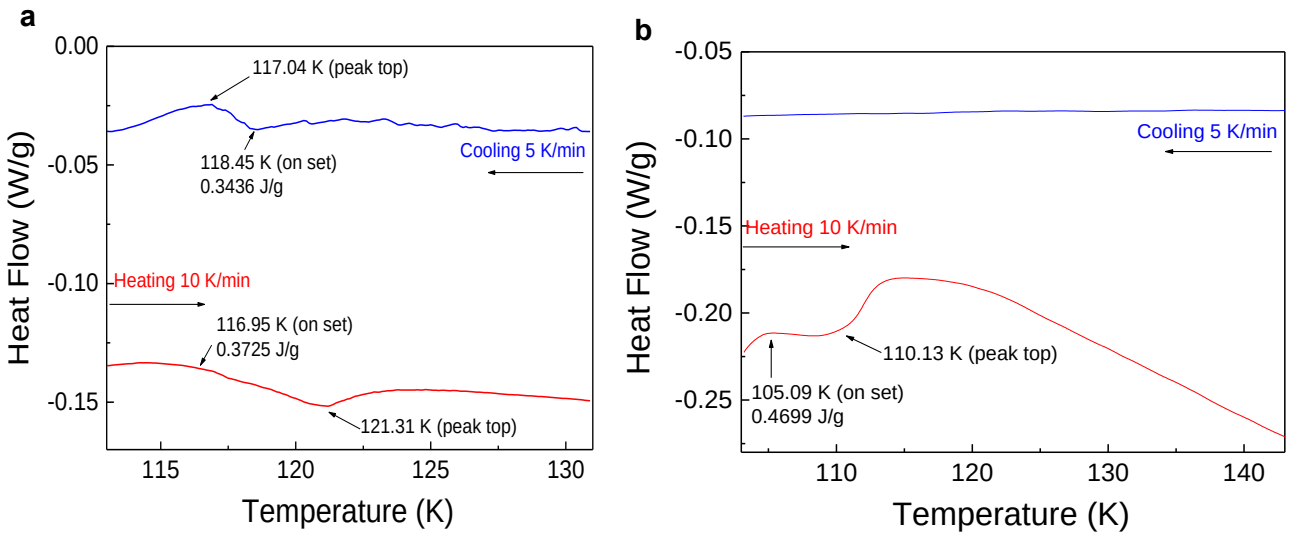


**Figure S5.** (a) DSC curves of **1oRR** on cooling/heating between 133 and 103 K (−140 and −170 °C). (b) DSC curves of a mixture of **1oRR** and **1cRR** with the ratio of 94 : 6 on cooling/heating between 83 and 143 K. Cooling and heating rates were 5 K /min and 10 K /min, respectively. (a) On cooling with 5 K /min, exothermic reaction was observed at 118.45 K (on set) and then heating at 10 K/min endothermic reaction was observed at 116.95 K (on set). These results indicate that phase transition from phase I to phase $III_{temp}$ occurred at 118.45 K on cooling, and phase transition from phase $III_{temp}$ to phase I occurred at 116.95 K on heating. (b) On cooling with 5 K /min, exothermic reaction was not observed till 90 K which is the lowest temperature by linear controlling mode of our DSC equipment. Once the measurement was stopped and the temperature was lowered to 83 K, and then heating was started with 10 K/min. Then, endothermic reaction was observed at 105.09 K (on set). In general, it is well-known that the decrease in the phase transition temperature caused by the contamination of the isomer by photoisomerization of diarylethene molecules.[4]

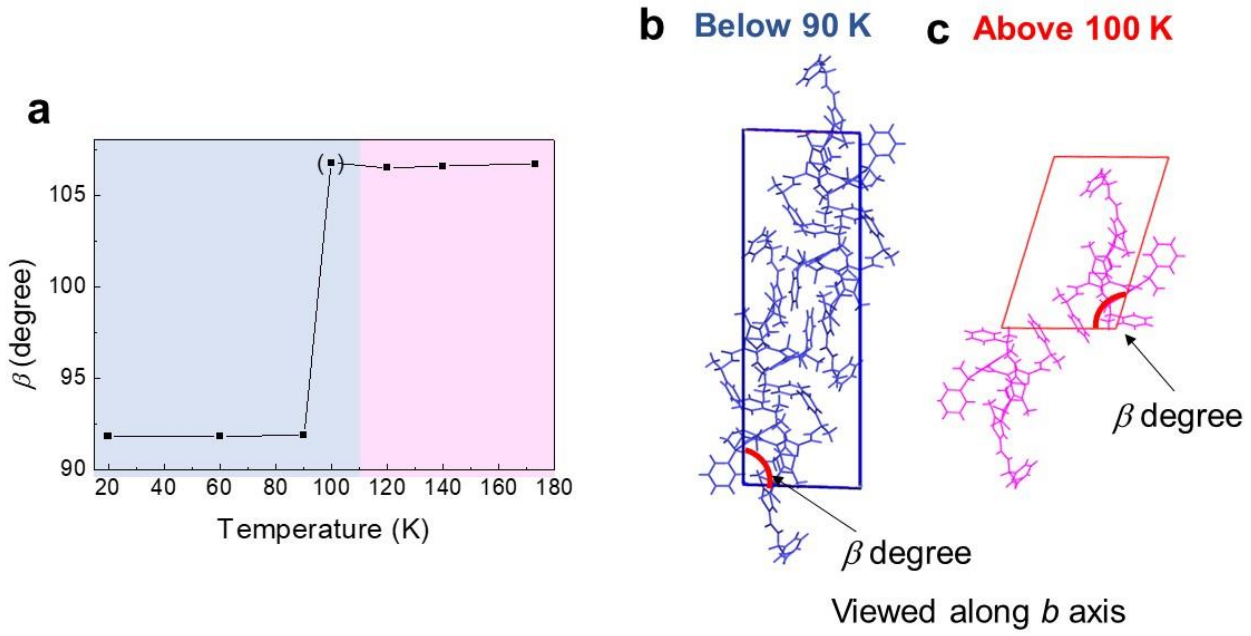


**Figure S6.** (a)The profile of $\beta$ angle of **1oRR** crystal during heating process from 20 K to 173 K with 10 K/min. (b) Unit cell after SCSC phase transition. (c) Unit cell before SCSC phase transition. Accompanied with changes of the ratio of rotamers of disordered phenyl rings in adjacent molecules in the crystal, $\beta$ angle dramatically changed from 91° to 106°. The $\beta$ angle at 100 K is 106° even though the temperature was below the thermal phase transition temperature of 117 K. This is because the diffraction spots attributed to the phase $III_{temp}$ were dim. The datum of (square symbol) is obtained by using another crystal.

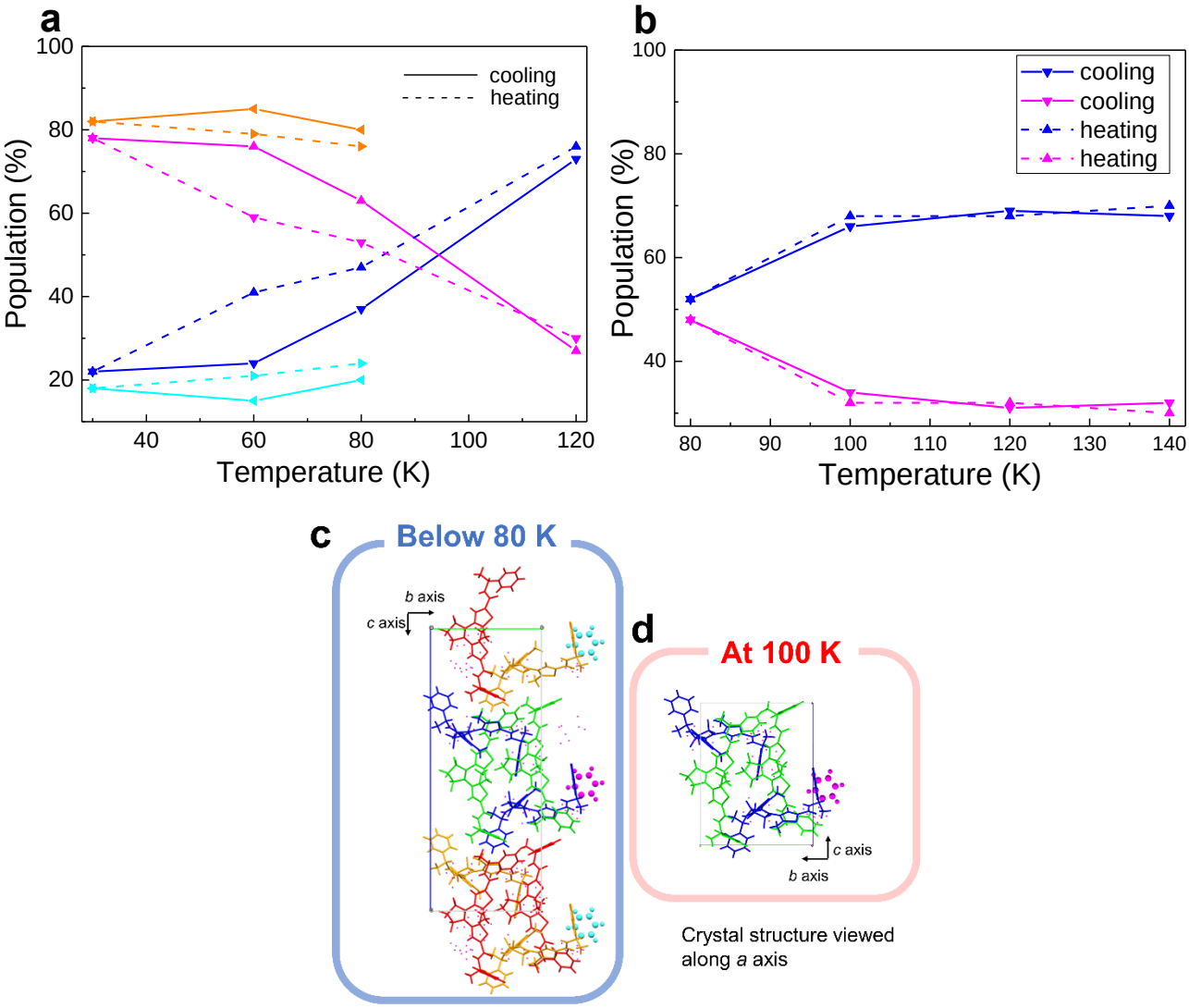


**Figure S7.** Hysteresis of population of phenyl-ring rotamers in monoclinic block crystal of **1oRR** by changing the temperature. Correlation diagram of disordered phenyl groups and measurement temperature (a) initially cooled down from 120 K to 30 K, followed by heating from 30 K to 120 K (b) initially cooled down from 140 K to 80 K, followed by heating from 80 K to 140 K. Solid line: cooling processes with rate of -5 K/min. Broken line: heating processes with 10 K/min. Blue line: populations of blue phenyl ring. Magenta line: populations of magenta phenyl ring. Orange line: population of orange phenyl ring. Pale blue line: population of pale blue phenyl ring (as shown in (c)). (c, d) The crystal structure of **1oRR** along *a* axis (c) below and (d) around SCSC phase transition temperature.

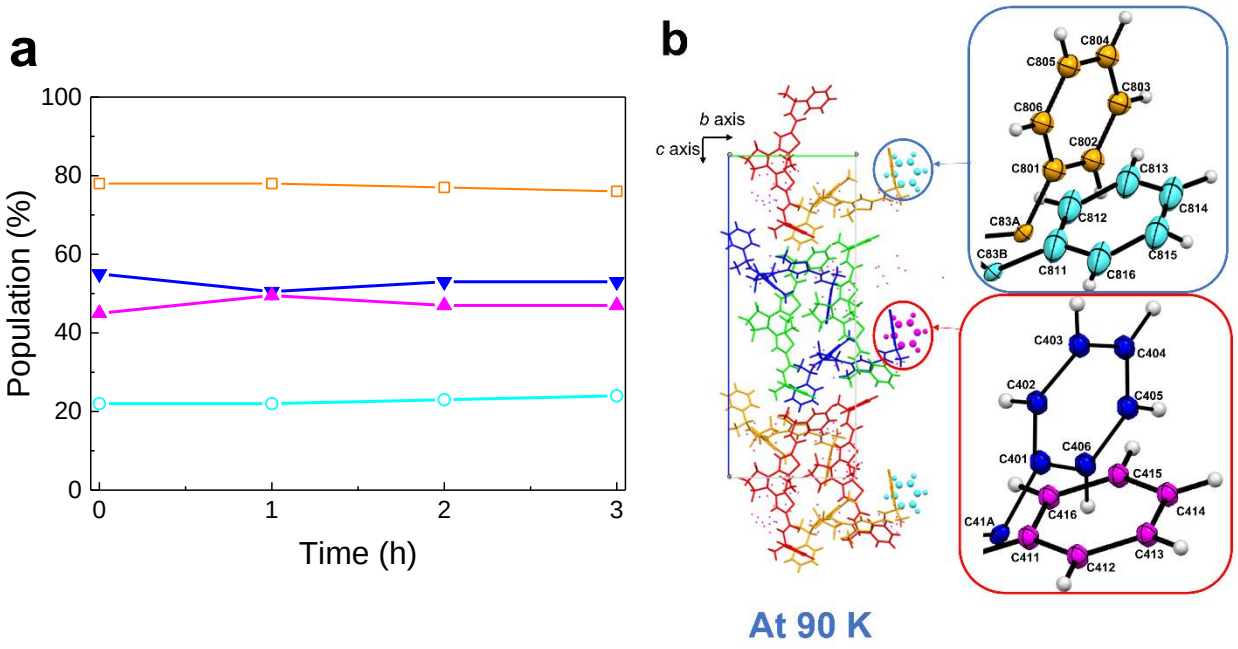


**Figure S8.** Result of disorder analysis of monoclinic block crystal of **1oRR** kept for 3 hours at 90 K. (a) The population of the rotamers of phenyl group of the crystal at 0, 1, 2, and 3 hours. The blue line indicates phenyl ring from C401 to C406, and the magenta line phenyl ring from C411 to C416. While the orange line indicates phenyl ring from C801 to C806, and the pale blue line phenyl ring from C811 to C816. (b) The view of crystal structure of **1oRR** along *a* axis. The population of disordered phenyl groups (magenta and pale blue) did not change even if the crystal was kept for 3 hours at 90 K. Thermal SCSC phase transition of **1oRR** is considered to be a martensitic-like transformation.

**Table S2.** The change in sizes of unit cells of monoclinic and orthorhombic crystal of **1oRR** from 120 K to 90 K.

| | **1oRR** (at 120 K) | **1oRR** (at 90 K) | **1oRR** (at 120 K) | **1oRR** (at 90 K) |
|---|---|---|---|---|
| crystal system | monoclinic | | orthorhombic | |
| $T$ / K | 120 (2) | 90 (2) | 120 (2) | 90 (2) |
| space group | $P2_1$ | $P2_1$ | $P2_12_12_1$ | $P2_12_12_1$ |
| $a$ / Å | 12.3036 (5) | 12.2772 (5) −0.21% | 12.3010 (9) | 12.2859 (8) −0.12% |
| $b$ / Å | 14.6207 (6) | 14.5882 (6) −0.22% | 14.4564 (10) | 14.4505 (9) −0.04% |
| $c$ / Å | 19.2792 (8) | 36.9888 (15) ($c'$/2 = 19.2900 +0.06%)*1 | 37.499 (3) | 37.464 (2) −0.09% |
| $\alpha$ / ° | 90 | 90 | 90 | 90 |
| $\beta$ / ° | 106.497 (8) | 91.924 (7) ($\beta'$ = 106.621 +0.12%)*2 | 90 | 90 |
| $\gamma$ / ° | 90 | 90 | 90 | 90 |
| $V$ / Å$^3$ | 3325.3 (3) | 6621.0 (5) ($V$/2 = 3310.5 −0.45%) | 6668.4 (9) | 6651.3 (7) −0.26% |
| $Z$ | 4 | 8 | 8 | 8 |
| $R_1$ ($I > 2\sigma(I)$) | 0.0584 | 0.0601 | 0.0900 | 0.0978 |
| $wR_2$ ($I > 2\sigma(I)$) | 0.1591 | 0.1619 | 0.2276 | 0.2501 |
| $R_1$ (all data) | 0.0605 | 0.0736 | 0.1441 | 0.1493 |
| $wR_2$ (all data) | 0.1616 | 0.1709 | 0.2656 | 0.2896 |
| CCDC | 1938361 | 1938360 | 1965757 | 1965756 |

*1: In order to compare the cell size before and after the phase transition, the half-length of the diagonal length between $c$ and $a$ axis ($c'$ axis) were compared.

*2: The $\beta'$-angle is obtained as an angle formed by the $a$-axis and the diagonal line of the $a$- and $c$-axes. The angle was compared with the $\beta$-angle before phase transition. The details are described in Figure S3.

When the orthorhombic crystal of **1oRR** was cooled down from 120 to 90 K, the volume contracted about 0.26%. The contraction ratio of orthorhombic crystal was almost the same as that of monoclinic crystal of **1oRR**. Therefore, it is considered that the volume contraction of monoclinic crystal of **1oRR** was due to cooling to low temperature.

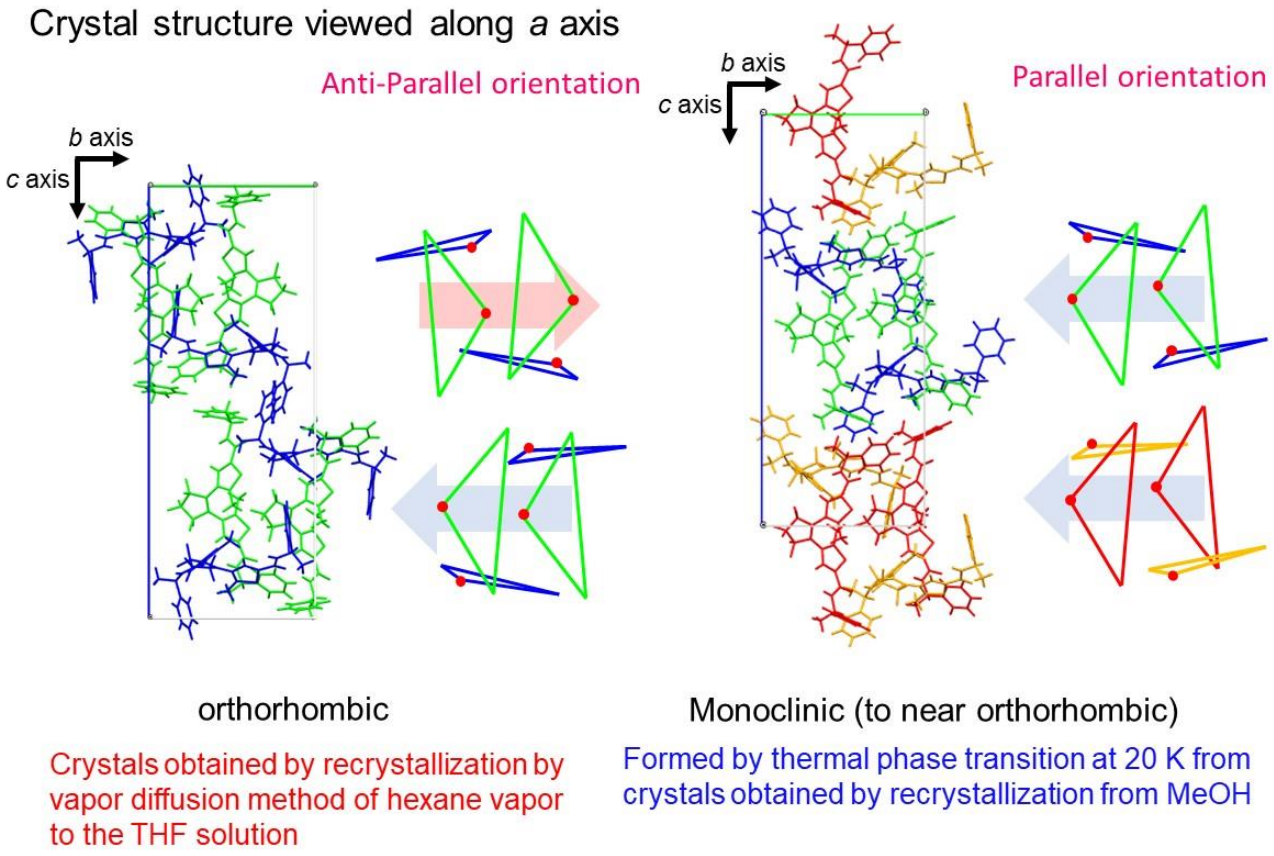


**Figure S9.** Comparison of orthorhombic and monoclinic crystal structures of **1oRR**. (a) The broad sword shaped crystal of orthorhombic prepared by vapor diffusion method of hexane vapor to the THF solution. (b) The block crystal of monoclinic prepared by recrystallization from MeOH (measured at 20 K). Focusing on the green and red conformers along *a* axis, the direction of short axis is anti-parallel in orthorhombic, while they are parallel in monoclinic.

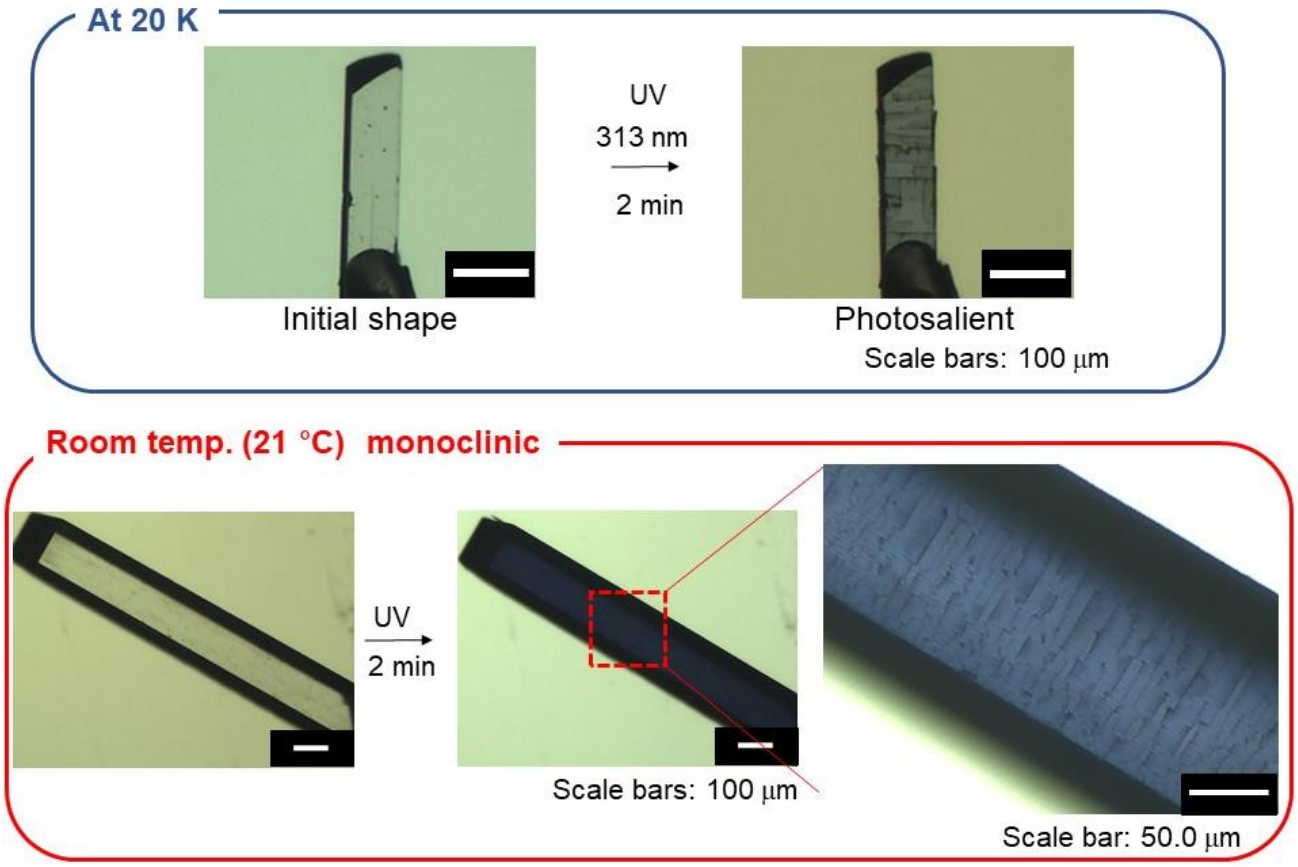


**Figure S10.** Photosalient phenomena of **1oRR** crystals obtained by recrystallization from MeOH (monoclinic block crystal). When the crystal was cooled to 20 K, cracks did not enter the crystal, but when subsequently irradiating ultraviolet light of 313 nm for 2 minutes in total, the surface had cracks. This phenomenon was also observed even at room temperature (21 °C).

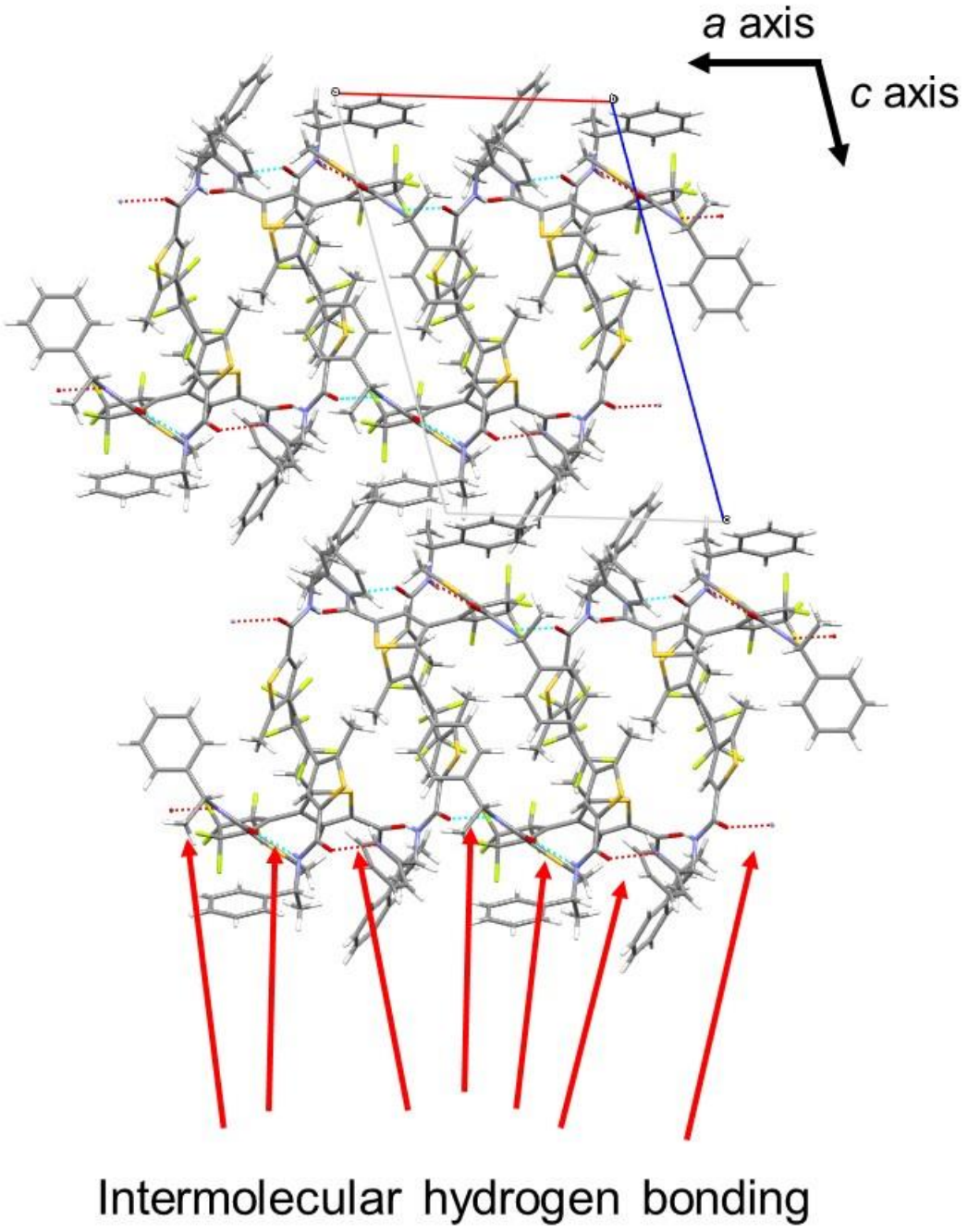


**Figure S11.** Crystalline structure of **1oRR** viewed along *b* axis at 173 K. Intermolecular hydrogen bonds are shown as red and pale-blue dotted lines (indicated by red arrows).

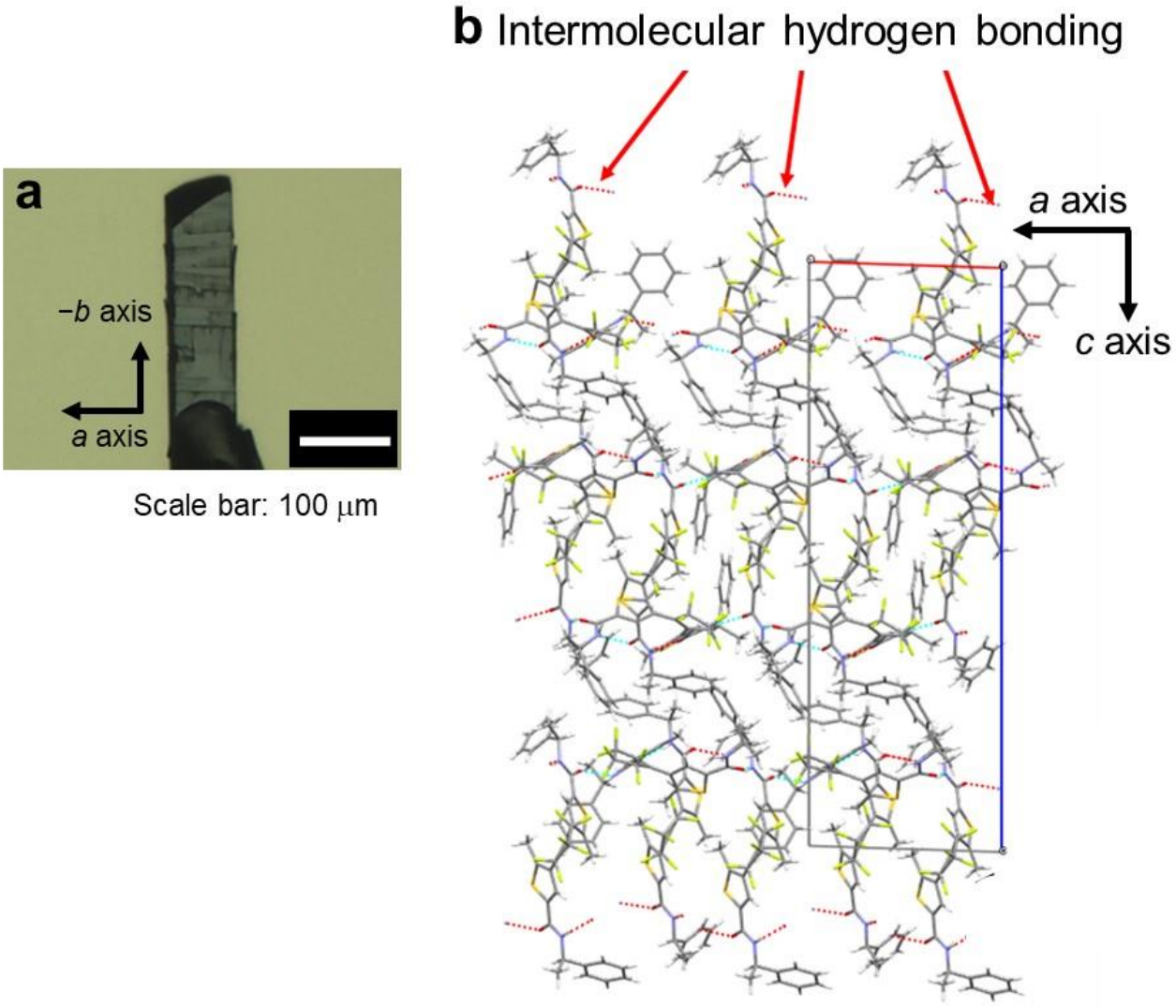


**Figure S12.** (a) Crystal after 2 min irradiation with 313 nm light, (b) Crystal structure as viewed along *b* axis. Intermolecular hydrogen bonds are indicated by dotted lines. After the experiment, there was some cracks generated along *a* axis. This is consistent with the direction of intermolecular hydrogen bonds, and it is considered that it is broken in the direction parallel to the hydrogen bonds, not to the vertical orientation with respect to the hard-to-break hydrogen bond.

**Table S3.** Crystal data of the broad sword shaped of **1oRR** which prepared by vapor diffusion method of hexane vapor to the THF solution.

| | **1oRR** (at 173 K) | **1oRR** (at 20 K) |
|---|---|---|
| $T$ / K | 173 (2) | 20 (2) |
| crystal system | orthorhombic | orthorhombic |
| space group | $P2_12_12_1$ | $P2_12_12_1$ |
| $a$ / Å | 12.3394 (16) | 12.1462 (4) −1.6% |
| $b$ / Å | 14.4779 (18) | 14.4267 (5) −0.35% |
| $c$ / Å | 37.612 (5) | 37.4462 (13) −0.44% |
| $\alpha$ / ° | 90 | 90 |
| $\beta$ / ° | 90 | 90 |
| $\gamma$ / ° | 90 | 90 |
| $V$ / Å$^3$ | 6719.3 (15) | 6561.7 (4) −2.3% |
| $Z$ | 8 | 8 |
| Density (g cm$^{-3}$) | 1.310 | 1.342 +2.4% |
| $R_1$ ($I > 2\sigma(I)$) | 0.0813 | 0.0567 |
| $wR_2$ ($I > 2\sigma(I)$) | 0.1947 | 0.1358 |
| $R_1$ (all data) | 0.1438 | 0.0660 |
| $wR_2$ (all data) | 0.2293 | 0.1424 |
| CCDC | 1938366 | 1965755 |

## References


1 K. Uchida, S. Sukata, Y. Matsuzawa, M. Akazawa, J. J. D. de Jong, N. Katsonis, Y. Kojima, S. Nakamura, J. Areephong, A. Meetsma, B. L. Feringa, *Chem. Commun.*, 2008, **5**, 326–328.

2 K. Uchida, M. Walko, J. J. D. de Jong, S. Sukata, S. Kobatake, A. Meetsma, J. van Esch, B. L. Feringa, *Org. Biomol. Chem.*, 2006, **4**, 1002–1006.

3 S. Kobatake, K. Uchida, E. Tsuchida, M. Irie, *Chem. Commun.*, **2002**, 2804–2805.

4 D. Kitagawa, K. Kawasaki, R. Tanaka, S. Kobatake, *Chem. Mater.*, 2017, **29**, 7524-7532.